TWMS J. App. and Eng. Math. V.16, N.8, 2026, pp. 989-1005

A COMPUTATIONAL ANALYSIS OF THE FACE INDEX OF CERTAIN GRAPH NETWORKS USING MULTIVARIATE REGRESSION

H.T. SHARATHKUMAR[1], POOJA N. SIMHA[2], N. NARAHARI[2], H.M. NAGESH[3,*] §

Abstract. Researchers have recently introduced a topological descriptor, called the face index, which quantifies the number of faces in a molecular network/compound to enhance efficiency by reducing computational time while improving the accuracy of chemical property calculations for chemical structures. It is observed that the face index provides valuable insights into the structural variations of different materials, offering a more generalized perspective compared to traditional vertex degree-based topological descriptors. This makes it a valuable tool for advancing research in chemistry and material science. Motivated by this, in the present study, we compute the face index for the chemical graphs of three significant networks namely the pentahexoctite, tetracyanobenzene and pyracyclene networks. Additionally, we perform a covariance analysis of this index with various degree-based topological indices for these networks. To further assess its predictability, we employ multivariate regression analysis, examining the relationship between the face index and these indices, which reveals a strong correlation between them.

Keywords: Topological indices, face index, degree-based topological indices, multivariate regression analysis.

AMS Subject Classification: 05C09, 05C92, 92E10.

1. Introduction

A graph is an ordered tuple $\mathbf{G} = (\mathcal{V}, \mathcal{E})$ consisting of a non-empty set $\mathcal{V}$, called the set of vertices and the set $\mathcal{E} \subseteq \mathcal{V} \times \mathcal{V}$, called the set of edges of $\mathbf{G}$. Chemical graph theory is a branch of mathematical chemistry that uses graph theory to model the behavior of chemicals. It involves employing a labeled graph that depicts the structure of a chemical

[1] Department of Studies and Research in Mathematics, Tumkur University, Tumakuru, Karnataka State, India.
e-mail: sharathkumkarht@tumkuruniversity.ac.in; https://orcid.org/0009-0004-2039-2862
[2] Department of Mathematics, University College of Science, Tumkur University, Tumakuru, Karnataka State, India.
e-mail: poojansimha99@gmail.com; https://orcid.org/0009-0001-8902-6420
e-mail: narahari@tumkuruniversity.ac.in; https://orcid.org/0000-0002-9243-840X
[3] Department of Science and Humanities, PES University, Bangalore, Karnataka State, India.
e-mail: nageshhm@pes.edu; https://orcid.org/0000-0001-9864-8937
* Corresponding author
§ Manuscript received: May 07, 2025; accepted: July 20, 2025.
TWMS Journal of Applied and Engineering Mathematics, Vol.16, No.8;

compound, with atoms represented by vertices and chemical bonds by edges. The characteristics of a chemical graph provide useful information about the corresponding chemical network. Its applications include the prediction of molecular physical characteristics like melting and boiling points, quantitative structure property relationships (QSPR) in quantitative form and examining complex chemical networks and topologies in chemistry. It is therefore utilized as an essential resource for comprehending molecular topology and the connection between chemical structure and chemical characteristics.

Recent advancements in chemical graph theory have expanded the scope of the field and have led to the development of new graph concepts in mathematical chemistry. These developments show that the field is seeing an increase in research and innovative approaches that improve our understanding of molecular structures and their properties. One of the most important graph parameters is the topological index, a numerical value that is inherited by a graph and can be associated with the chemical reactivity, biological activity and physical characteristics of the individual chemical molecule.

In general, a vertex-degree-based (VDB) topological index can be written as

$$\mathcal{TI}(\mathbf{G}) = \sum_{\mathbf{uv}\in\mathcal{E}(\mathbf{G})} \mathrm{f}(d(\mathbf{u}), d(\mathbf{v}))$$

where $d(\mathbf{u})$ represents the number of vertices adjacent with the vertex $\mathbf{u}$, called the degree of $\mathbf{u}$, in the graph $\mathbf{G}$. Some of the commonly known vertex-degree-based topological indices are the Zagreb index [8, 3], Randić index [19], forgotten index [8], atom-bond connectivity index [7], geometric-arithmetic index [25], harmonic index [29], arithmetic-geometric index [22], Sombor index [9], atom-bond sum-connectivity index [2] and reverse Sombor index [14].

The effectiveness and applications of a topological index are significantly influenced by its computational complexity and discriminating capabilities. In recent studies, researchers have introduced a novel topological descriptor called the face index to improve the efficiency of determining physical characteristics such as energy, melting point, boiling point, enthalpy, entropy etc., of different (molecular) chemical structures without relying on complex computational methods.

The face index [12] is a novel topological index that characterizes planar graphs, i.e., graphs that can be drawn on a plane without crossing any of their edges. A region surrounded by graph edges is referred to as one of its faces. In particular, an internal face refers to a region enclosed by the edges of the planar graph and an external face refers to the unbounded region, forming the graph's external boundary. The face index of a planar graph represents the sum of the degrees of the vertices lying on the boundary of all its distinct faces. As seen in literature, the face index provides valuable details regarding the complicated nature and connectivity of the planar graphs and is therefore widely used in conjunction with other topological indices to analyze and compare graphs, understand their properties and develop algorithms for a range of applications in material science, chemistry, network research and other fields by minimizing computational time. The computational complexity of the face index increases with the number of faces in the graph and the complexity of the molecular structure. However, computing the face index with symmetric configurations becomes easier due to the uniform face degree sums across layers so that the study of face index is very significant in understanding the structural properties of a chemical network/compound, particularly with reference to its symmetry. For related work on the face index, we refer [12, 13, 27, 15, 16, 17, 6]. As observed in these studies, computing the face index of chemical structures and networks plays an important role in analyzing their structural properties.

TABLE 1. Definitions of topological indices discussed

SL. NO.	INDEX	MATHEMATICAL EXPRESSION
1	FACE INDEX [12]	$\mathrm{FI}(\mathbf{G}) = \sum_{\mathbf{f}\in\mathcal{F}(\mathbf{G})} d(\mathbf{f}) = \sum_{\mathbf{v}\in\mathbf{f},\mathbf{f}\in\mathcal{F}(\mathbf{G})} d(\mathbf{v})$
2	GEOMETRIC-ARITHMETIC INDEX [25]	$\mathrm{GA}(\mathbf{G}) = \sum_{\mathbf{uv}\in\mathcal{E}(\mathbf{G})} \frac{2\sqrt{d(\mathbf{u})\cdot d(\mathbf{v})}}{d(\mathbf{u})+d(\mathbf{v})}$
3	ARITHMETIC-GEOMETRIC INDEX [22]	$\mathrm{AG}(\mathbf{G}) = \sum_{\mathbf{uv}\in\mathcal{E}(\mathbf{G})} \frac{d(\mathbf{u})+d(\mathbf{v})}{2\sqrt{d(\mathbf{u})\cdot d(\mathbf{v})}}$
4	FORGOTTEN INDEX [8]	$\mathrm{F}(\mathbf{G}) = \sum_{\mathbf{uv}\in\mathcal{E}(\mathbf{G})} \left(d(\mathbf{u})^2 + d(\mathbf{v})^2\right)$
5	ATOM-BOND CONNECTIVITY INDEX [7]	$\mathrm{ABC}(\mathbf{G}) = \sum_{\mathbf{uv}\in\mathcal{E}(\mathbf{G})} \sqrt{\frac{d(\mathbf{u})+d(\mathbf{v})-2}{d(\mathbf{u})\cdot d(\mathbf{v})}}$
6	ATOM-BOND SUM-CONNECTIVITY INDEX [2]	$\mathrm{ABS}(\mathbf{G}) = \sum_{\mathbf{uv}\in\mathcal{E}(\mathbf{G})} \sqrt{\frac{d(\mathbf{u})+d(\mathbf{v})-2}{d(\mathbf{u})+d(\mathbf{v})}}$
7	SOMBOR INDEX [9]	$\mathrm{SO}(\mathbf{G}) = \sum_{\mathbf{uv}\in\mathcal{E}(\mathbf{G})} \sqrt{d(\mathbf{u})^2 + d(\mathbf{v})^2}$
8	REVERSE SOMBOR INDEX [14]	$\mathrm{RSO}(\mathbf{G}) = \sum_{\mathbf{uv}\in\mathcal{E}(\mathbf{G})} \sqrt{c(\mathbf{u})^2 + c(\mathbf{v})^2}$

In this article, we compute the face index of the chemical networks, namely pentahexoctite ($\mathcal{PH}(\beta_1,\beta_2)$), tetracyanobenzene ($\mathcal{TCNB}(\beta_1,\beta_2)$) and pyracyclene ($\mathcal{PC}(\beta_1,\beta_2)$). Further, we perform a covariance analysis of this index with some of the commonly known degree-based topological indices, including the forgotten index, atom-bond connectivity index, geometric-arithmetic index, arithmetic-geometric index, atom-bond sum-connectivity index, Sombor index and the reverse Sombor index with reference to these networks. Also, we analyze the best predictability of the face index in terms of these degree-based topological indices by means of multivariate regression analysis. For related work on these degree-based topological indices and their applicability, we refer [2, 10, 9, 8, 14, 13, 23].

2. PRELIMINARIES

The two-dimensional structure of a molecular graph can be represented by the graph $\mathbf{G} = (\mathcal{V}, \mathcal{E}, \mathcal{F})$, in which $\mathcal{V}(\mathbf{G})$ represents the collection of vertices, $\mathcal{E}(\mathbf{G})$ the collection of edges and $\mathcal{F}(\mathbf{G})$ the collection of faces. Every graph taken into account here is a simple, connected and planar graph. A face $\mathbf{f}$ is said to be incident with an edge $\mathbf{e}$ if $\mathbf{e}$ is the edge that surrounds the face $\mathbf{f}$. Similarly, $\mathbf{f}$ is said to be incident with a vertex $\mathbf{v}$ if $\mathbf{v}$ is at the end of one of those incident edges. The degree of a vertex $\mathbf{v}$, denoted as $d(\mathbf{v})$, is the number of edges that are adjacent to it. Further, $d(\mathbf{f})$, called the degree of the face $\mathbf{f}$, is defined as the sum of the degrees of all the vertices incident with $\mathbf{f}$ and $\mathbf{f}_k$ represents a face with degree k. The reverse vertex degree of a vertex $\mathbf{v}$, denoted $c(\mathbf{v})$, is defined as $c(\mathbf{v}) = \Delta - d(\mathbf{v}) + 1$, where Δ is the maximum degree of any vertex in $\mathbf{G}$.

Table 1 contains the list of definitions of all the topological indices discussed in this article.

3. RESULTS AND DISCUSSION

3.1. **Pentahexoctite Network.** The graphene [28] is a two-dimensional form of a graphite structure with fascinating characteristics such as energy level alignment and adjustable band gaps. It is gaining major attention in its applications due to its diverse range of allotropes with amazing electrical, chemical, thermal and electronic properties. A particular kind of graphene network is the pentahexoctite network.

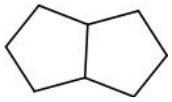

FIGURE 1. Pentahexoctite unit structure

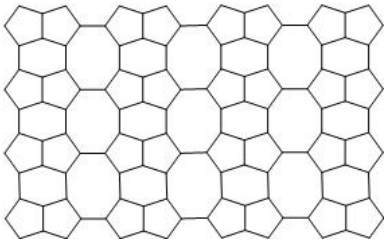

FIGURE 2. $\mathcal{PH}(4,4)$

TABLE 2. Partition of edges in $\mathcal{PH}(\beta_1, \beta_2)$

Edge type	**Cardinality**
$(2,2)$	4
$(2,3)$	$4\beta_1 + 8\beta_2 - 8$
$(1,3)$	$12\beta_1\beta_2 - 5\beta_1 - 10\beta_2 + 4$

Pentahexoctite is formed by octagons, pentagons and hexagonal structures. It possesses mechanical strength similar to graphene and can be rolled into stable nanotubes, with chirality influencing both its mechanical and electronic characteristics. In addition to this, it is a planar stable network. These unique properties make it a strong candidate for nano-electronic applications. As a result, it has been recognized as a promising addition to the growing family of novel 2D carbon allotropes, particularly in the domain of electronic technologies [21]. Therefore researchers are very much interested in the study of pentahexoctite networks. $\mathcal{PH}(\beta_1, \beta_2)$ represents the pentahexoctite network of dimension (β_1, β_2), where β_1 represents number of rows and β_2 represents number of columns. The unit structure of pentahexoctite network and the representation of $\mathcal{PH}(\beta_1, \beta_2)$ when $\beta_1, \beta_2 = 4$ are shown in Figure 1 and Figure 2 respectively. The calculation shows that the graph of $\mathcal{PH}(\beta_1, \beta_2)$ has $8\beta_1\beta_2$ vertices and $12\beta_1\beta_2 - \beta_1 - 2\beta_2$ edges. The edge partition of $\mathcal{PH}(\beta_1, \beta_2)$ is given in Table 2.

The following theorem provides the expression for the face index of $\mathcal{PH}(\beta_1, \beta_2)$.

Theorem 3.1. *Let $\mathbf{G} = \mathcal{PH}(\beta_1, \beta_2)$ be the pentahexoctite network of dimension (β_1, β_2). Then, for $\beta_1, \beta_2 \geq 1$, the face index of $\mathcal{PH}(\beta_1, \beta_2)$ is given by*

$$\mathrm{FI}(\mathcal{PH}(\beta_1, \beta_2)) = \begin{cases} 46\beta_2 - 4 & \text{if } \beta_1 = 1 \\ 72\beta_1\beta_2 - 10\beta_1 - 20\beta_2 & \text{if } \beta_1 > 1. \end{cases}$$

Proof. The face index for the given network is calculated by considering the following two cases.

Case 1: $\beta_1 = 1$.

In this case, $\mathcal{PH}(1, \beta_2)$ has two distinct internal faces $\mathbf{f}_{12}$ and $\mathbf{f}_{13}$ along with an exterior face $\mathbf{f}^{\infty}$. More information on the internal face partition of $\mathcal{PH}(1, \beta_2)$ in different dimensions has been provided in Table 3. Similarly, Table 4 illustrates the degree of the external face, or degree sum of the vertices incident on the external face in different dimensions. Using the information obtained from Table 3 and Table 4, the face index of $\mathcal{PH}(1, \beta_2)$ can be calculated as follows:

$$\begin{aligned} \mathrm{FI}(\mathcal{PH}(1, \beta_2)) &= \sum_{\mathbf{v} \in \mathbf{f}_k} d(\mathbf{v}) = \sum_{\mathbf{v} \in \mathbf{f}_{12}} d(\mathbf{v}) \; + \sum_{\mathbf{v} \in \mathbf{f}_{13}} d(\mathbf{v}) \; + \sum_{\mathbf{v} \in \mathbf{f}^{\infty}} d(\mathbf{v}) \\ &= 46\beta_2 - 4. \end{aligned}$$

TABLE 3. Internal face partition of $\mathcal{PH}(1, \beta_2)$

Dimension	$\lvert\mathbf{f}_{12}\rvert$	$\lvert\mathbf{f}_{13}\rvert$
$(1,1)$	2	0
$(1,2)$	2	2
$(1,3)$	2	4
$(1,4)$	2	6
$\vdots$	$\vdots$	$\vdots$
$(1,\beta_2)$	2	$2\beta_2 - 2$

TABLE 4. External face degree of $\mathcal{PH}(1, \beta_2)$

Dimension	$(1,1)$	$(1,2)$	$(1,3)$	$(1,4)$	$\ldots$	$(1,\beta_2)$
External face degree	18	38	58	78	$\ldots$	$20\beta_2 - 2$

TABLE 5. Internal face partition of $\mathcal{PH}(\beta_1, \beta_2)$

Dimension	$\lvert\mathbf{f}_{13}\rvert$	$\lvert\mathbf{f}_{14}\rvert$	$\lvert\mathbf{f}_{15}\rvert$	$\lvert\mathbf{f}_{18}\rvert$	$\lvert\mathbf{f}_{24}\rvert$
$(2,2)$	4	8	0	2	1
$(2,3)$	4	12	0	3	2
$(3,2)$	4	10	2	4	2
$(3,3)$	4	14	4	6	4
$\vdots$	$\vdots$	$\vdots$	$\vdots$	$\vdots$	$\vdots$
(β_1,β_2)	4	$4\beta_2 + 2\beta_1 - 4$	$2\beta_1\beta_2 - 2\beta_1 - 4\beta_2 + 4$	$\beta_1\beta_2 - \beta_2$	$\beta_1\beta_2 - \beta_1 - \beta_2 + 1$

TABLE 6. External face degree of $\mathcal{PH}(\beta_1, \beta_2)$

Dimension	$(2,2)$	$(2,3)$	$(3,2)$	$(3,3)$	$\ldots$	(β_1,β_2)
External face degree	60	86	76	102	$\ldots$	$16\beta_1 + 26\beta_2 - 24$

Case 2: $\beta_1 > 1$.
In this case, $\mathcal{PH}(\beta_1, \beta_2)$ has five distinct internal faces of the form $\mathbf{f}_{13}$, $\mathbf{f}_{14}$, $\mathbf{f}_{15}$, $\mathbf{f}_{18}$ and $\mathbf{f}_{24}$ along with an external face $\mathbf{f}^{\infty}$. More information on the internal face partition of $\mathcal{PH}(\beta_1, \beta_2)$ in different dimensions has been provided in Table 5. Now, we shall calculate the internal face degree of $\mathcal{PH}(\beta_1, \beta_2)$ i.e., degree sum of the vertices incident on the internal faces. Using Table 5, we have

$$\begin{aligned}\sum_{\mathbf{v}\in\mathbf{f}_k} d(\mathbf{v}) &= \sum_{\mathbf{v}\in\mathbf{f}_{13}} d(\mathbf{v}) + \sum_{\mathbf{v}\in\mathbf{f}_{14}} d(\mathbf{v}) + \sum_{\mathbf{v}\in\mathbf{f}_{15}} d(\mathbf{v}) + \sum_{\mathbf{v}\in\mathbf{f}_{18}} d(\mathbf{v}) + \sum_{\mathbf{v}\in\mathbf{f}_{24}} d(\mathbf{v}) \\ &= 4(13) + (4\beta_2 + 2\beta_1 - 4)(14) + (2\beta_1\beta_2 - 2\beta_1 - 4\beta_2 + 4)(15) + (\beta_1\beta_2 - \beta_2)(18) \\ &\quad + (\beta_1\beta_2 - \beta_1 - \beta_2 + 1)(24) \\ &= 72\beta_1\beta_2 - 26\beta_1 - 46\beta_2 + 24.\end{aligned}$$

Similarly, Table 6 illustrates the degree of the external face under the second case. From Table 6, the external face degree is given by

$$\sum_{\mathbf{v}\in\mathbf{f}^{\infty}} d(\mathbf{v}) = 16\beta_1 + 26\beta_2 - 24.$$

Therefore, the face index of $\mathcal{PH}(\beta_1, \beta_2)$ is given by

$$\begin{aligned}\mathrm{FI}(\mathcal{PH}(\beta_1, \beta_2)) &= \sum_{\mathbf{v}\in\mathbf{f}_k} d(\mathbf{v}) + \sum_{\mathbf{v}\in\mathbf{f}^\infty} d(\mathbf{v}) \\ &= 72\beta_1\beta_2 - 26\beta_1 - 46\beta_2 + 24 + 16\beta_1 + 26\beta_2 - 24 \\ &= 72\beta_1\beta_2 - 10\beta_1 - 20\beta_2.\end{aligned}$$

□

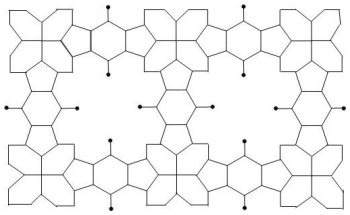

FIGURE 3. $\mathcal{TCNB}(1, 2)$

3.2. **Tetracyanobenzene Network.** Metal-organic frameworks [1] or MOFs are a special kind of compounds that have captured the attention of researchers because of their special properties and wide range of applications. In a gram of material, this combination produces a highly porous fabric with an enormous internal surface area that is often close to the size of a football field. MOFs are used in many different applications. The storage and separation of fuel is one of their most significant uses. Because of their high porosity, MOFs have the ability to keep large amounts of gases, such as methane or hydrogen, which makes them promising components for clean energy systems.

Tetracyanobenzene metal-organic framework [1] is one of the prominent MOFs, with high porosity, electrical conductivity and thermal stability obtained by reacting metal salt with $\mathcal{TCNB}$ in a solvent. It is a two-dimensional network of transition metal ions such as Ti, V, Fe, Co, Ni, Cu and Zn that has a distinct structure that ranges from metallic to half metallic. Ti, V, Cr and Mn produce half-metallic MOFs, which exhibit a gap in one spin direction, whereas metals like Ni, Fe, Zn and Co produce fully metallic structures. The configuration in the $\mathcal{TCNB}(\beta_1, \beta_2)$ network exhibits a screening effect, especially with Ti, V, Cr and Co, wherein spin-polarized electrons from the surrounding organic ligands play a major impact on the characteristics of $\mathcal{TCNB}(\beta_1, \beta_2)$ networks.

Organic charger-transfer materials have been widely studied over the past few decades due to their promising applications as wavelength-tunable fluorophores and their beneficial roles in organic transistors and photovoltaics. Their easy fabrication through solution or vapor deposition, along with the ability to modify constituent molecules, allows precise control over band gaps and triplet spin dynamics. Similarly, organic luminescent materials have attracted considerable attention for their outstanding properties, with many luminescent organic molecules serving as sensors, whiteners, colorants and active emitters in light-emitting diodes. Tetracyanobenzene ($\mathcal{TCNB}$) is a well known charge-transfer material in this domain [24, 18] and has therefore drawn a lot of attention of researchers.

The tetracyanobenzene network of dimension (β_1, β_2) [1], represented by the symbol $\mathcal{TCNB}(\beta_1, \beta_2)$, has a chemical structure made up of $\beta_1 \geq 1$ horizontal and $\beta_2 \geq 1$ vertical expansions as shown in Figure 3. With $25\beta_1 + 25\beta_2 + 33\beta_1\beta_2 + 17$ vertices and $32\beta_1 + 32\beta_2 + 44\beta_1\beta_2 + 20$ edges, $\mathcal{TCNB}(\beta_1, \beta_2)$ has a graphical design. Table 7 shows the edge partition of $\mathcal{TCNB}(\beta_1, \beta_2)$. Using this information, we propose the following result giving the expression of the face index of $\mathcal{TCNB}(\beta_1, \beta_2)$.

TABLE 7. Partition of edges in $\mathcal{TCNB}(\beta_1, \beta_2)$

Edge type	**Cardinality**
$(1,3)$	$2\beta_1 + 2\beta_2 + 4\beta_1\beta_2$
$(2,3)$	$8\beta_1 + 8\beta_2 + 8\beta_1\beta_2 + 8$
$(2,2)$	$4\beta_1 + 4\beta_2 + 8$
$(3,3)$	$14\beta_1 + 14\beta_2 + 28\beta_1\beta_2$
$(3,4)$	$4\beta_1 + 4\beta_2 + 4\beta_1\beta_2 + 4$

TABLE 8. Internal face partition of $\mathcal{TCNB}(\beta_1, \beta_2)$

Dimension	$\lvert\mathbf{f}_{15}\rvert$	$\lvert\mathbf{f}_{16}\rvert$	$\lvert\mathbf{f}_{17}\rvert$	$\lvert\mathbf{f}_{18}\rvert$	$\lvert\mathbf{f}_{72}\rvert$
$(1,1)$	8	4	8	8	1
$(1,2)$	14	4	12	15	2
$(2,2)$	24	4	16	28	4
$(2,3)$	34	4	20	41	6
$(3,3)$	48	4	24	60	9
$(3,4)$	62	4	28	79	12
$\vdots$	$\vdots$	$\vdots$	$\vdots$	$\vdots$	$\vdots$
(β_1, β_2)	$4\beta_1\beta_2 + 2\beta_1 + 2\beta_2$	4	$4\beta_1 + 4\beta_2$	$6\beta_1\beta_2 + \beta_1 + \beta_2$	$\beta_1\beta_2$

TABLE 9. External face degree of $\mathcal{TCNB}(\beta_1, \beta_2)$

Dimension	$(1,1)$	$(1,2)$	$(2,2)$	$(2,3)$	$(3,3)$	$(3,4)$	...	(β_1, β_2)
Pendent vertices	4	6	8	10	12	14	...	$2\beta_1 + 2\beta_2$
External face degree	144	198	252	306	360	414	...	$54\beta_1 + 54\beta_2 + 36$

Theorem 3.2. *Let* $\mathbf{G} = \mathcal{TCNB}(\beta_1, \beta_2)$ *be the tetracyanobenzene network of dimension* (β_1, β_2)*. Then, for* $\beta_1, \beta_2 \geq 1$*, the face index of* $\mathcal{TCNB}(\beta_1, \beta_2)$ *is given by*

$$\mathrm{FI}(\mathcal{TCNB}(\beta_1, \beta_2)) = 240\beta_1\beta_2 + 170\beta_1 + 170\beta_2 + 100.$$

Proof. In addition to an external face $\mathbf{f}^{\infty}$, $\mathcal{TCNB}(\beta_1, \beta_2)$ has five distinct internal faces, namely $\mathbf{f}_{15}$, $\mathbf{f}_{16}$, $\mathbf{f}_{17}$, $\mathbf{f}_{18}$ and $\mathbf{f}_{72}$. More information on the internal face partition of $\mathcal{TCNB}(\beta_1, \beta_2)$ in each dimension has been provided in Table 8. Using the information given in Table 8, we get the internal face degree of $\mathcal{TCNB}(\beta_1, \beta_2)$ i.e., degree sum of the vertices incident on the internal faces as

$$\begin{aligned}\sum_{\mathbf{v}\in\mathbf{f}_k} d(\mathbf{v}) &= \sum_{\mathbf{v}\in\mathbf{f}_{15}} d(\mathbf{v}) + \sum_{\mathbf{v}\in\mathbf{f}_{16}} d(\mathbf{v}) + \sum_{\mathbf{v}\in\mathbf{f}_{17}} d(\mathbf{v}) + \sum_{\mathbf{v}\in\mathbf{f}_{18}} d(\mathbf{v}) + \sum_{\mathbf{v}\in\mathbf{f}_{72}} d(\mathbf{v}) \\ &= (4\beta_1\beta_2 + 2\beta_1 + 2\beta_2)(15) + (4)(16) + (4\beta_1 + 4\beta_2)(17) \\ &\quad + (6\beta_1\beta_2 + \beta_1 + \beta_2)(18) + (\beta_1\beta_2)(72) \\ &= 240\beta_1\beta_2 + 116\beta_1 + 116\beta_2 + 64.\end{aligned}$$

Similarly, Table 9 illustrates the degree of the external face in each dimension. From Table 9, we have

$$\sum_{\mathbf{v}\in\mathbf{f}^{\infty}} d(\mathbf{v}) = 54\beta_1 + 54\beta_2 + 36.$$

TABLE 10. Partition of edges in $\mathcal{PC}(\beta_1, \beta_2)$

Edge type	Cardinality
$(2, 2)$	$2\beta_1 + 2\beta_2$
$(2, 3)$	$4\beta_1 + 4\beta_2$
$(1, 3)$	$21\beta_1\beta_2 - 8\beta_1 - 8\beta_2$

The face index of $\mathcal{TCNB}(\beta_1, \beta_2)$ can thus be calculated as follows:

$$\begin{aligned}\mathrm{FI}(\mathcal{TCNB}(\beta_1, \beta_2)) &= \sum_{\mathbf{v}\in\mathbf{f}_k} d(\mathbf{v}) + \sum_{\mathbf{v}\in\mathbf{f}^{\infty}} d(\mathbf{v}) \\ &= 240\beta_1\beta_2 + 116\beta_1 + 116\beta_2 + 64 + 54\beta_1 + 54\beta_2 + 36 \\ &= 240\beta_1\beta_2 + 170\beta_1 + 170\beta_2 + 100.\end{aligned}$$

□

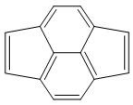

FIGURE 4. Pyracyclene chemical structure

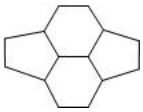

FIGURE 5. Pyracyclene unit structure

3.3. **Pyracyclene Network.** Pyracyclene [28] is a type of graphene having a polymerized planar structure with a tetragonal lattice having the chemical formula $C_{14}H_8$. The massless fermion carrier velocities of this Dirac semi-metal can be adjusted to $7 \times 10^5 m/s$ by adjusting the tensile strain. It plays a prominent role in designing novel graphene allotropes with high stability [11] and it is used as a bridge to build stable N-heteroacene derivatives [26]. Thus, networks of pyracyclenes [28] have greater significance in the field of chemistry.

The pyracyclene network $\mathcal{PC}(\beta_1, \beta_2)$ is of dimension (β_1, β_2), where β_1 represents the number of rows and β_2 represents the number of columns. Figure 5 is its unit structure whereas Figure 6 is the structure of this network when $\beta_1 = \beta_2 = 4$. The graph of $\mathcal{PC}(\beta_1, \beta_2)$ has $14\beta_1\beta_2$ vertices and $21\beta_1\beta_2 - 2\beta_1 - 2\beta_2$ edges. The edge partition of $\mathcal{PC}(\beta_1, \beta_2)$ is given in Table 10. We propose the following result giving the expression of the face index of $\mathcal{PC}(\beta_1, \beta_2)$.

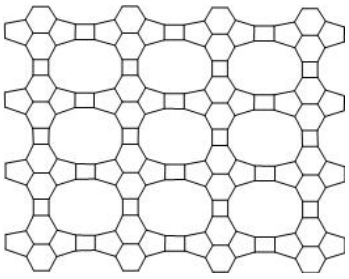

FIGURE 6. $\mathcal{PC}(4, 4)$

TABLE 11. Internal face partition of $\mathcal{PC}(\beta_1, 1)$

Dimension	$\lvert\mathbf{f}_{12}\rvert$	$\lvert\mathbf{f}_{13}\rvert$	$\lvert\mathbf{f}_{16}\rvert$	$\lvert\mathbf{f}_{18}\rvert$
$(1,1)$	0	2	2	0
$(2,1)$	1	4	2	2
$(3,1)$	2	6	2	4
$(4,1)$	3	8	2	6
$\vdots$	$\vdots$	$\vdots$	$\vdots$	$\vdots$
$(\beta_1,1)$	β_1-1	$2\beta_1$	2	$2(\beta_1-1)$

TABLE 12. External face degree of $\mathcal{PC}(\beta_1, 1)$

Dimension	$(1,1)$	$(2,1)$	$(3,1)$	$(4,1)$	...	$(\beta_1,1)$
External face degree	28	60	92	124	...	$32\beta_1-4$

Theorem 3.3. *Let* $\mathbf{G} = \mathcal{PC}(\beta_1, \beta_2)$ *be the pyracyclene network of dimension* (β_1, β_2). *Then, for* $\beta_1, \beta_2 \geq 1$, *the face index of* $\mathcal{PC}(\beta_1, \beta_2)$ *is given by*

$$\mathrm{FI}(\mathcal{PC}(\beta_1,\beta_2)) = \begin{cases} 106\beta_1 - 20 & \text{if } \beta_2 = 1 \text{ and } \beta_1 \geq 1 \\ 106\beta_2 - 20 & \text{if } \beta_1 = 1 \text{ and } \beta_2 \geq 1 \\ 126\beta_1\beta_2 - 20\beta_1 - 20\beta_2 & \text{if } \beta_1, \beta_2 \geq 2. \end{cases}$$

Proof. In this network, the face index is calculated by considering three different cases. The cases are discussed as follows:

Case 1: $\beta_2 = 1$ and $\beta_1 \geq 1$.

In this case, $\mathcal{PC}(\beta_1, 1)$ has four distinct internal faces in the form $\mathbf{f}_{12}, \mathbf{f}_{13}, \mathbf{f}_{16}$ and $\mathbf{f}_{18}$ along with an external face $\mathbf{f}^{\infty}$. More information on the internal face partition of $\mathcal{PC}(\beta_1, 1)$ in different dimensions has been provided in Table 11. From Table 11, we get the internal face degree as

$$\begin{aligned} \sum_{\mathbf{v}\in\mathbf{f}_k} d(\mathbf{v}) &= \sum_{\mathbf{v}\in\mathbf{f}_{12}} d(\mathbf{v}) + \sum_{\mathbf{v}\in\mathbf{f}_{13}} d(\mathbf{v}) + \sum_{\mathbf{v}\in\mathbf{f}_{16}} d(\mathbf{v}) + \sum_{\mathbf{v}\in\mathbf{f}_{18}} d(\mathbf{v}) \\ &= (\beta_1 - 1)12 + (2\beta_1)13 + 2(16) + (2\beta_1 - 2)18 \\ &= 74\beta_1 - 16. \end{aligned}$$

Similarly, the external face degree in different dimensions can be seen in Table 12.

From Table 12, we have the external face degree

$$\sum_{\mathbf{v}\in\mathbf{f}^{\infty}} d(\mathbf{v}) = 32\beta_1 - 4.$$

Thus, the face index of $\mathcal{PC}(\beta_1, 1)$ is given by

$$\begin{aligned} \mathrm{FI}(\mathcal{PC}(\beta_1,1)) &= \sum_{\mathbf{v}\in\mathbf{f}_k} d(\mathbf{v}) + \sum_{\mathbf{v}\in\mathbf{f}^{\infty}} d(\mathbf{v}) \\ &= 106\beta_1 - 20. \end{aligned}$$

Case 2: $\beta_1 = 1$ and $\beta_2 \geq 1$.

In this case, $\mathcal{PC}(1, \beta_2)$ contains four different internal faces $\mathbf{f}_{12}$, $\mathbf{f}_{13}$, $\mathbf{f}_{15}$ and $\mathbf{f}_{16}$ along with an external face $\mathbf{f}^{\infty}$. Table 13 gives information about the internal face partition of $\mathcal{PC}(1, \beta_2)$ in different dimensions. Similarly, the external face degree i.e., degree sum of the vertices incident on the external face in different dimensions can be seen in Table 14. From Table 13, we get the internal face degree as

TABLE 13. Internal face partition of $\mathcal{PC}(1,\beta_2)$

Dimension	$\lvert\mathbf{f}_{12}\rvert$	$\lvert\mathbf{f}_{13}\rvert$	$\lvert\mathbf{f}_{15}\rvert$	$\lvert\mathbf{f}_{16}\rvert$
$(1,1)$	0	2	0	2
$(1,2)$	1	2	2	4
$(1,3)$	2	2	4	6
$(1,4)$	3	2	6	8
$\vdots$	$\vdots$	$\vdots$	$\vdots$	$\vdots$
$(1,\beta_2)$	β_2-1	2	$2(\beta_2-1)$	$2(\beta_2)$

TABLE 14. External face degree of $\mathcal{PC}(1,\beta_2)$

Dimension	$(1,1)$	$(1,2)$	$(1,3)$	$(1,4)$	$\ldots$	$(1,\beta_2)$
External face degree	28	60	92	124	$\ldots$	$32\beta_2-4$

$$\begin{aligned}\sum_{\mathbf{v}\in\mathbf{f}_k} d(\mathbf{v}) &= \sum_{\mathbf{v}\in\mathbf{f}_{12}} d(\mathbf{v}) + \sum_{\mathbf{v}\in\mathbf{f}_{13}} d(\mathbf{v}) + \sum_{\mathbf{v}\in\mathbf{f}_{15}} d(\mathbf{v}) + \sum_{\mathbf{v}\in\mathbf{f}_{16}} d(\mathbf{v})\\ &= (\beta_2-1)12 + (2)13 + (2\beta_2-2)(15) + (2\beta_2)16\\ &= 74\beta_2 - 16.\end{aligned}$$

From Table 14, we have the external face degree

$$\sum_{\mathbf{v}\in\mathbf{f}^\infty} d(\mathbf{v}) = 32\beta_2 - 4.$$

Thus, the face index of $\mathcal{PC}(1,\beta_2)$ becomes

$$\begin{aligned}\mathrm{FI}(\mathcal{PC}(1,\beta_2)) &= \sum_{\mathbf{v}\in\mathbf{f}_k} d(\mathbf{v}) + \sum_{\mathbf{v}\in\mathbf{f}^\infty} d(\mathbf{v})\\ &= 74\beta_2 - 16 + 32\beta_2 - 4\\ &= 106\beta_2 - 20.\end{aligned}$$

Case 3: $\beta_1,\beta_2 \geq 2$.
In this case, $\mathcal{PC}(\beta_1,\beta_2)$ contains six different internal faces $\mathbf{f}_{12}$, $\mathbf{f}_{13}$, $\mathbf{f}_{15}$, $\mathbf{f}_{16}$, $\mathbf{f}_{18}$ and $\mathbf{f}_{36}$ along with an external face $\mathbf{f}^\infty$. Table 15 gives information about the internal face partition of $\mathcal{PC}(\beta_1,\beta_2)$ in different dimensions. From Table 15, we get the internal face degree as

$$\begin{aligned}\sum_{\mathbf{v}\in\mathbf{f}_k} d(\mathbf{v}) &= \sum_{\mathbf{v}\in\mathbf{f}_{12}} d(\mathbf{v}) + \sum_{\mathbf{v}\in\mathbf{f}_{13}} d(\mathbf{v}) + \sum_{\mathbf{v}\in\mathbf{f}_{15}} d(\mathbf{v}) + \sum_{\mathbf{v}\in\mathbf{f}_{16}} d(\mathbf{v})\\ &\quad + \sum_{\mathbf{v}\in\mathbf{f}_{18}} d(\mathbf{v}) + \sum_{\mathbf{v}\in\mathbf{f}_{36}} d(\mathbf{v})\\ &= (2\beta_1\beta_2 - \beta_1 - \beta_2)12 + (2\beta_1)(13) + (2\beta_1\beta_2 - 2\beta_1)(15) + (2\beta_2)(16)\\ &\quad + (2\beta_1\beta_2 - 2\beta_2)(18) + (\beta_1\beta_2 - \beta_1 - \beta_2 + 1)(36)\\ &= 126\beta_1\beta_2 - 52\beta_1 - 52\beta_2 + 36.\end{aligned}$$

Similarly, the external face degree in different dimensions can be seen in Table 16. From Table 16, we have the external face degree

$$\sum_{\mathbf{v}\in\mathbf{f}^\infty} d(\mathbf{v}) = 32\beta_1 + 32\beta_2 - 36.$$

TABLE 15. Internal face partition of $\mathcal{PC}(\beta_1, \beta_2)$

Dimension	$\lvert\mathbf{f}_{12}\rvert$	$\lvert\mathbf{f}_{13}\rvert$	$\lvert\mathbf{f}_{15}\rvert$	$\lvert\mathbf{f}_{16}\rvert$	$\lvert\mathbf{f}_{18}\rvert$	$\lvert\mathbf{f}_{36}\rvert$
$(1,1)$	0	2	0	2	0	0
$(1,2)$	0	2	2	4	0	0
$(1,3)$	0	2	4	6	0	0
$(1,4)$	0	2	6	8	0	0
$(1,5)$	0	2	8	10	0	0
$(2,1)$	1	4	0	2	2	0
$(2,2)$	4	4	4	4	4	1
$(2,3)$	7	4	8	6	6	2
$(2,4)$	10	4	12	8	8	3
$(2,5)$	13	4	16	10	10	4
$(3,1)$	2	6	0	2	4	0
$(3,2)$	7	6	6	4	8	2
$(3,3)$	12	6	12	6	12	4
$(3,4)$	17	6	18	8	16	6
$(3,5)$	22	6	24	10	20	8
$\vdots$	$\vdots$	$\vdots$	$\vdots$	$\vdots$	$\vdots$	$\vdots$
(β_1, β_2)	$2\beta_1\beta_2 - \beta_1 - \beta_2$	$2\beta_1$	$2\beta_1\beta_2 - 2\beta_1$	$2\beta_2$	$2\beta_1\beta_2 - 2\beta_2$	$\beta_1\beta_2 - \beta_1 - \beta_2 + 1$

TABLE 16. External face degree of $\mathcal{PC}(\beta_1, \beta_2)$

Dimension	$(1,1)$	$(1,2)$	$(1,3)$	$(2,1)$	$(2,2)$	...	(β_1, β_2)
External face degree	28	60	92	60	92	...	$32\beta_1 + 32\beta_2 - 36$

The face index of the $\mathcal{PC}(\beta_1, \beta_2)$ is then given by

$$\begin{aligned} \mathrm{FI}(\mathcal{PC}(\beta_1, \beta_2)) &= \sum_{\mathbf{v}\in\mathbf{f}_k} d(\mathbf{v}) + \sum_{\mathbf{v}\in\mathbf{f}^\infty} d(\mathbf{v}) \\ &= 126\beta_1\beta_2 - 52\beta_1 - 52\beta_2 + 36 + 32\beta_1 + 32\beta_2 - 36 \\ &= 126\beta_1\beta_2 - 20\beta_1 - 20\beta_2. \end{aligned}$$

□

4. Covariance and Regression Analysis

4.1. **Covariance Analysis.** In this section, for each chemical network discussed in this article, we calculate the different degree-based topological indices, namely the arithmetic-geometric index, geometric-arithmetic index, atom-bond connectivity index, forgotten index, atom-bond sum-connectivity index, Sombor index and the reverse Sombor index and observe their correlation with the face index. The covariance of the face index with other degree-based topological indices is established by plotting the graphs for the covariance table of each chemical network. The face index, atom-bond sum-connectivity index (ABS), geometric-arithmetic index (GA), Sombor index and reverse Sombor index is plotted in the first graph, while the atom-bond connectivity index (ABC), arithmetic-geometric index (AG), forgotten index and face index is plotted in the second graph.

4.2. **Multivariate Regression Analysis.** This section presents two multivariate regression analysis models [12, 20] that are used to determine the best predictability of the face index in terms of degree-based topological indices for each chemical network. The general form of the multivariate regression models will be

$$Y = \beta_1(T_1) + \beta_2(T_2) + \beta_3(T_3) + \cdots + \beta_n(T_n) + r$$

where Y corresponds to some property, r is the regression constant and β_i are regression coefficients for the topological descriptors T_i. The multivariate models and parameters

TABLE 17. Covariance table for $\mathbf{G} = \mathcal{PH}(\beta_1, \beta_2)$

(β_1, β_2)	FI($\mathbf{G}$)	SO($\mathbf{G}$)	RSO($\mathbf{G}$)	GA($\mathbf{G}$)	AG($\mathbf{G}$)	ABC($\mathbf{G}$)	F($\mathbf{G}$)	ABS($\mathbf{G}$)
(2, 2)	228	162.341	78.2035	41.6767	42.3299	28.8088	636	33.1849
(3, 3)	558	396.526	168.676	98.4343	99.5774	67.2941	1602	79.2224
(4, 4)	1032	732.535	293.089	179.192	180.825	121.779	3000	144.856
(5, 5)	1650	1170.37	451.444	283.949	286.072	192.265	4830	230.085
(6, 6)	2412	1710.02	643.74	412.707	415.32	278.75	7092	334.91
(7, 7)	3318	2351.5	869.977	565.464	568.567	381.235	9786	459.332
(8, 8)	4368	3094.8	1130.15	742.222	745.815	499.72	12912	603.349
(9, 9)	5562	3939.93	1424.27	942.98	947.062	634.206	16470	766.962
(10, 10)	6900	4886.88	1752.33	1167.74	1172.31	784.691	20460	950.171
(11, 11)	8382	5935.65	2114.34	1416.49	1421.56	951.176	24882	1152.98
(12, 12)	10008	7.86.25	2510.28	1689.25	1694.8	1133.66	29736	1375.38
(13, 13)	11778	8338.67	2940.16	1986.01	1992.05	1332.15	35022	1617.37
(14, 14)	13692	9692.91	3403.99	2306.77	2313.3	1546.63	40470	1878.97
(15, 15)	15750	11149	3901.75	2651.52	2658.55	1777.12	46890	2160.15
(16, 16)	17952	12706.9	4433.46	3020.28	3027.79	2023.6	53472	2460.94
(17, 17)	20298	14366.6	4999.11	3413.04	3421.04	2286.09	60846	2781.32
(18, 18)	22788	16128.1	55988.7	3829.8	3838.29	2564.57	67932	3121.3
(19, 19)	25422	17991.5	6232.23	4270.56	4279.54	2859.06	75810	3480.87
(20, 20)	28200	19956.7	6899.7	4735.31	4744.78	3169.54	84120	3860.04

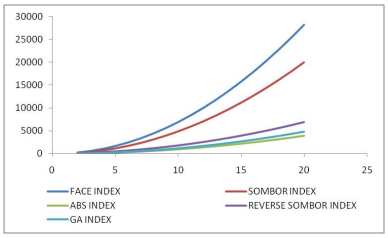

FIGURE 7. Covariance graph for $\mathcal{PH}(\beta_1, \beta_2)$-1

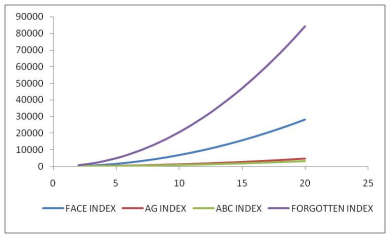

FIGURE 8. Covariance graph for $\mathcal{PH}(\beta_1, \beta_2)$-2

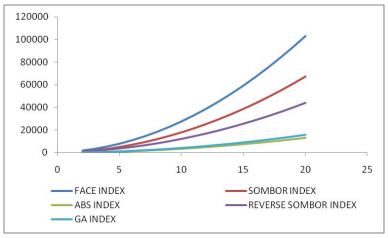

FIGURE 9. Covariance graph $\mathcal{TCNB}(\beta_1, \beta_2)$-1

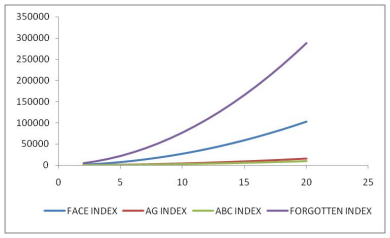

FIGURE 10. Covariance graph $\mathcal{TCNB}(\beta_1, \beta_2)$-2

relevant to each model for each chemical network are provided in the following tables. Here, Y is the face index, X_1 the Sombor index, X_2 the reverse Sombor index, X_3 the forgotten index, Z_1 the atom-bond connectivity index and Z_2 the atom-bond sum-connectivity index of the graph, a_i and b_i the regression coefficients and a_4, b_3 the regression constants for Model-1 and Model-2 respectively for the above mentioned topological indices.
In Tables 21 and 23, MSE denotes the mean squared error, r the correlation coefficient, SSE the sum of squared error, Std. error the standard error and Sign. F the significance

TABLE 18. Covariance table for $\mathbf{G} = \mathcal{TCNB}(\beta_1, \beta_2)$

(β_1, β_2)	FI($\mathbf{G}$)	SO($\mathbf{G}$)	RSO($\mathbf{G}$)	GA($\mathbf{G}$)	AG($\mathbf{G}$)	ABC($\mathbf{G}$)	F($\mathbf{G}$)	ABS($\mathbf{G}$)
$(2, 2)$	1740	1194.95	881.32	291.248	292.62	196.588	4972	234.682
$(3, 3)$	3280	2221.65	1583.4	535.973	535.59	358.853	9328	433.238
$(4, 4)$	5300	3558.34	2483.68	853.364	849.735	568.397	15020	691.016
$(5, 5)$	7800	5205	3582.15	1243.42	1235.05	825.22	22048	1008.02
$(6, 6)$	10780	7161.64	4878.81	1706.15	1691.55	1129.32	30412	1384.24
$(7, 7)$	14240	9428.26	6373.66	2241.54	2219.22	1480.7	40112	1819.68
$(8, 8)$	18180	12004.9	8066.7	2849.59	2818.07	1879.36	51148	2314.35
$(9, 9)$	26000	14891.4	9957.94	3530.32	3488.09	2325.3	63520	2868.23
$(10, 10)$	27500	18088	12047.4	4283.71	4229.28	2818.52	77228	3481.34
$(11, 11)$	32880	21594.5	14335	5109.77	5041.66	3359.02	92272	4153.67
$(12, 12)$	38740	25411	16820.8	6008.49	5925.2	3946.79	108652	4885.22
$(13, 13)$	45080	29537.5	19504.8	6979.88	6879.92	81.85	126368	5676
$(14, 14)$	51900	33974	22387	8023.94	7905.82	5264.18	145420	6525.99
$(15, 15)$	59200	38720.4	25467.4	9140.66	9002.89	5993.8	165808	7435.21
$(16, 16)$	66980	43776.9	28746	10330	10171.1	6770.69	187532	8403.65
$(17, 17)$	75240	49143.3	32222.8	11592.1	11410.6	7594.86	210592	9431.31
$(18, 18)$	83980	54819.7	35897.7	12926.8	12721.2	8466.31	234988	10518.2
$(19, 19)$	93200	60806	39770.9	14334.2	14102.9	9385.04	260720	11664.3
$(20, 20)$	102900	67102.4	43842.2	15814.3	15555.9	10351	287788	12869.6

TABLE 19. Covariance table for $\mathbf{G} = \mathcal{PC}(\beta_1, \beta_2)$

(β_1, β_2)	FI($\mathbf{G}$)	SO($\mathbf{G}$)	RSO($\mathbf{G}$)	GA($\mathbf{G}$)	AG($\mathbf{G}$)	ABC($\mathbf{G}$)	F($\mathbf{G}$)	ABS($\mathbf{G}$)
$(2, 2)$	424	300.934	131.944	75.6767	76.3299	51.6372	1208	60.5082
$(3, 3)$	1014	718.687	287.011	176.515	177.495	119.456	2964	142.202
$(4, 4)$	1856	1314.63	501.475	319.353	320.66	215.274	5440	258.18
$(5, 5)$	2950	2088.77	775.336	504.192	505.825	339.093	8690	408.467
$(6, 6)$	4296	3041.09	1108.59	731.03	732.99	490.912	12696	593.039
$(7, 7)$	5894	4171.61	1501.25	999.869	1002.15	670.78	17458	811.904
$(8, 8)$	7744	5480.32	1953.3	1310.71	1313.32	878.549	22976	1065.06
$(9, 9)$	9846	6967.21	2464.75	1663.55	1666.48	1114.37	29250	1352.51
$(10, 10)$	12200	8632.3	3035.6	2058.38	2061.65	1378.19	36280	1674.26
$(11, 11)$	14806	10475.6	3665.84	2495.22	2498.81	1670	44066	2030.29
$(12, 12)$	17664	12497.1	4355.48	2974.06	2977.98	1989.82	52608	2420.62
$(13, 13)$	20774	14696.7	5104.52	3494.9	3499.14	2337.64	61906	2845.24
$(14, 14)$	24136	17074.6	5912.95	4057.74	4062.31	2713.46	71960	3304.16
$(15, 15)$	15750	19630.6	6780.78	4662.58	4667.47	3117.28	82770	3797.37
$(16, 16)$	31616	22364.9	7708.01	5309.41	5314.64	3549.1	94336	4324.87
$(17, 17)$	35734	25277.3	8694.63	5998.25	6003.8	4008.92	106658	4886.66
$(18, 18)$	40164	28367.9	9740.66	6729.09	6734.97	44496.74	119736	5482.75
$(19, 19)$	44726	31636.7	10846.1	7501.93	7508.13	5012.55	133570	6113.12
$(20, 20)$	49600	35083.7	12010.9	8316.77	8323.3	556.37	148160	6777.8

TABLE 20. Table of multivariate regression models

Model	**Multivariate regression equation**
1	$Y = a1 \cdot X_1 + a2 \cdot X_2 + a3 \cdot X_3 + a4$
2	$Y = b1 \cdot Z_1 + b2 \cdot Z_2 + b3$

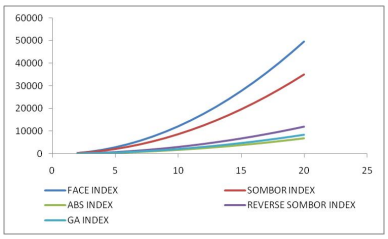

FIGURE 11. Covariance graph for $\mathcal{PC}(\beta_1, \beta_2)$-1

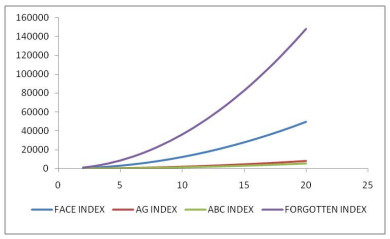

FIGURE 12. Covariance graph for $\mathcal{PC}(\beta_1, \beta_2)$-2

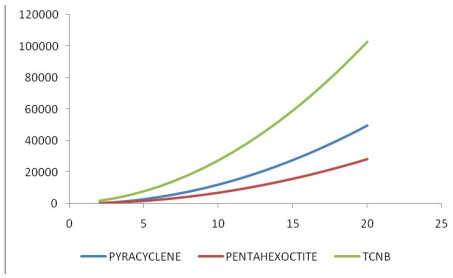

FIGURE 13. Face index comparison graph

TABLE 21. Parameters supporting multivariate regression Model-1

Network	r	r^2	**Std. error**	SSE	F	**Sig.** F	MSE
$\mathcal{PH}(\beta_1, \beta_2)$	1	1	0.00129	2.498×10^{-5}	0.896×10^{14}	0.198×10^{-103}	1.665×10^{-6}
$\mathcal{TCNB}(\beta_1, \beta_2)$	1	1	0.00814	0.00099	9.440×10^{13}	8.7214×10^{100}	6.632×10^{-5}
$\mathcal{PC}(\beta_1, \beta_2)$	1	1	0.00287	0.00012	1.8×10^{14}	7×10^{-102}	8.29×10^{-6}

TABLE 22. Table of multivariate regression models used for considered chemical networks

Networks	**Model**	**Multivariate regression equations**
$\mathcal{PH}(\beta_1, \beta_2)$	1	$Y = 0.044169X_1 + 0.529170X_2 + 0.281346X_3 + 0.509871$
	2	$Y = -9.266511Z_1 + 14.914509Z_2 + 0.013820$
$\mathcal{TCNB}(\beta_1, \beta_2)$	1	$Y = -0.057005X_1 - 0.431542X_2 + 0.436526X_3 + 18.036866$
	2	$Y = -18.477887Z_1 + 22.856684Z_2 + 8.398978$
$\mathcal{PC}(\beta_1, \beta_2)$	1	$Y = 0.064564X_1 + 0.547828X_2 + 0.275073X_3 - 0.001809$
	2	$Y = -9.246196Z_1 + 14.897950Z_2 + 0.001044$

F respectively. In regression analysis, the correlation coefficient (r) is a numerical value ranging from -1 to $+1$, representing the strength and direction of the relationship between independent and dependent variables. Generally, an absolute correlation coefficient value greater than 0.7 signifies a strong relationship, while values ranging from 0.5 to 0.7 suggest a moderate relationship between the variables. Moreover, for the regression model to best fit the data, Mean Squared Error (MSE), Sum of Squared Errors (SSE) and the Sign. F should all be low, very close to zero. Additionally, the F value should be greater than 2.5 to ensure the reliability of the model.

5. CONCLUSION

In this article, we have computed the face index for the pentahexoctite ($\mathcal{PH}(\beta_1, \beta_2)$), tetracyanobenzene ($\mathcal{TCNB}(\beta_1, \beta_2)$) and pyracyclene ($\mathcal{PC}(\beta_1, \beta_2)$) networks. The face

TABLE 23. Parameters supporting multivariate regression Model-2

Network	r	r^2	**Std. error**	SSE	F	**Sig.** F	MSE
$\mathcal{PH}(\beta_1, \beta_2)$	1	1	0.04964	0.03942	2.935×10^{11}	3.0422×10^{-85}	0.00246
$\mathcal{TCNB}(\beta_1, \beta_2)$	1	1	0.08940	0.12788	1.175×10^{12}	4.614×10^{-90}	0.00779
$\mathcal{PC}(\beta_1, \beta_2)$	1	1	0.03265	0.01706	2.1×10^{12}	4.51×10^{-92}	0.00106

index of each of the chemical networks mentioned above has been compared to degree-based topological indices such as the geometric-arithmetic index, arithmetic-geometric index, atom-bond connectivity index, forgotten index, atom-bond sum-connectivity index, Sombor index and the reverse Sombor index. Furthermore, for each chemical network, we have proposed two multivariate regression models to determine the best predictability of the face index in terms of other degree-based topological indices. In the regression analysis performed in the study, the correlation coefficient for each model is numerically close to 1 with the corresponding F values sufficiently large and the value of significance F very close to zero. Therefore, it can be concluded that, with regard to the multivariate regression models examined in the current study, the face index is best predictable in terms of the other degree-based topological indices.

6. Future Work

This study presents a comparative analysis of the face index with some of the degree-based topological indices considering some specific networks. Further analysis of this index, by considering indices based on other parameters such as distance and spectrum, might explain the significance of this index. In literature, various graph energies have been introduced based on topological indices. Some of the commonly known graph energies are the Zagreb energy, Randić energy and Sombor energy. One can extend this idea to define the face energy of a planar graph and study its properties and perform QSPR and/or QSAR analyses of various chemical compounds and networks using this parameter.

Computing the face index is relatively straightforward for chemical structures represented in two-dimensional form, with symmetric configurations calculations are even easier due to uniform face degree sums across layers. However, the face index cannot be computed directly for all types of biomolecular graphs or nanostructures, as it is strictly applicable to planar structures and cannot be used for three-dimensional molecular graphs. Nevertheless, Shell Theory [4, 5], an established method in the literature, offers a way to convert both $2D$ and $3D$ chemical structures into $2D$ graphical representations, enabling the computation of face indices even for complex structures. With the application of Shell Theory, one may explore methods to compute the face index of any kind molecular graphs/network. The concept of face index could also be further extended to weighted or labeled graphs, by reformulating its expression by incorporating weights/labels of edges into the vertex degrees. Further, a comparative analysis of the face index and face energy with other energies can also be carried out.

7. Novelty Statement

This article presents a novel computational approach to analyze the newly introduced face index by means of computing it for significant graph networks and comparing it with some of the commonly studied degree-based topological indices using covariance analysis. Further, the multivariate analysis assesses the predictability of the face index with these indices and establishes a strong correlation between them. This provides a distinct perspective, providing meaningful insights into the structural variations of various

networks/compounds compared to the existing studies on traditional degree-based topological indices.

References

[1] Al-Dayel, I., Nadeem, M. F. and Khan, M. A., (2024), Topological analysis of tetracyanobenzene metal–organic framework, Sci. Rep., 14(1), 1789.

[2] Ali, A., Furtula, B., Redzepovic, I. and Gutman, I., (2022), Atom-bond sum-connectivity index, J. Math. Chem., 60, pp. 2081–2093.

[3] Austel, V., Balaban, A. T., Bonchev, D., Charton, M., Fujita, T., Iwamura, H. and Mekenyan, O., (1983), Topological indices for structure-activity correlations in steric effects in drug design, Springer, pp. 21-55.

[4] Carrera, E., (1995), A class of two-dimensional theories for anisotropic multilayered plates analysis, Atti Accad. Sci. Memor. Sci. Fisich., 19, pp. 48-87.

[5] Carrera, E., (1999), Multilayered shell theories accounting for layerwise mixed description, Part 1: governing equations, AIAA J., 37(9), pp. 1107-1116.

[6] Ding, S., Qureshi, M. I., Shah, S. F., Fahad, A., Jamil, M. K. and Liu, J. B., (2021), Face index of nanotubes and regular hexagonal lattices, Int. J. Quantum Chem., 121(19), 26761.

[7] Estrada, E., Torres, L., Rodriguez, L. and Gutman, I., (1998), An atom-bond connectivity index: modelling the enthalpy of formation of alkanes, Indian J. Chem., 37A, pp. 849-855.

[8] Gutman, I. and Trinajstic, N., (1972), Graph theory and molecular orbitals. Total π-electron energy of alternant hydrocarbons, Chem. Phys. Lett., 17(4), pp. 535-538.

[9] Gutman, I., Geometric approach to degree-based topological indices: Sombor indices, (2021), MATCH Commun. Math. Comput. Chem., 86(1), pp. 11-16.

[10] Gowtham, K. J., Narahari, N., Sooryanarayana, B. and Cangul, I. N., (2024), Some properties of the novel topological graph index atom-bond sum-connectivity index, Montes Taurus J. Pure Appl. Math., 6(3), pp. 418-427.

[11] Huang, W., Hou, L., Song, Y. and Chen, G., (2023), Novel Graphene Allotropes Designed by Polymerizing Pyracyclene Molecules, J. Phys. Chem. C, 127(39), pp. 19814-19824.

[12] Jamil, M. K., Imran, M. and Abdul Sattar, K., (2020), Novel face index for benzenoid hydrocarbons, Mathematics, 8(3), 312.

[13] Luo, R., Dawood, K., Jamil, M. K. and Azeem, M., (2023), Some new results on the face index of certain polycyclic chemical networks, Math. Biosci. Eng., 2, pp. 8031-8048.

[14] Narahari, N., Manohar, T., Sooryanarayana, B. and Gutman, I., (2022), Reverse Sombor index, Bull. Int. Math. Virtual Inst., 12(2), pp. 267-272.

[15] Negi, S., Lal, S. and Bhat, V. K., (2023), On boron nanotubes and their face index, MAMS, 31(27), pp. 9232–9240.

[16] Negi, S. and Bhat, V. K., (2024), Face index of silicon carbide structures: An alternative approach, Silicon, 16(16), pp. 5865-5876.

[17] Negi, S. and Bhat, V. K., (2025), On carbon nanocones $CNC_m[n]$ and their face index, Phosphorus, Sulfur and Silicon and the Related Elements, 200(2), pp. 144-151.

[18] Ng, W., Zhang, S., Wu, H., Nevjestic, I., White, A. J. and Oxborrow, M., (2021), Exploring the triplet spin dynamics of the charge-transfer co-crystal phenazine/1, 2, 4, 5-tetracyanobenzene for potential use in organic maser gain media, J. Phys. Chem. C, 125(27), pp. 14718-14728.

[19] Randić, M., (1975), On characterization of molecular branching, J. Am. Chem. Soc., 97, pp. 6609-6615.

[20] Sarkarai, D. and Desikan, K., (2023), QSPR/QSAR analysis of some eccentricity based topological descriptors of antiviral drugs used in COVID-19 treatment via D$\in$-polynomials, Math. Biosci. Eng., 20(9), pp. 17272-17295.

[21] Sharma, B. R., Manjanath, A. and Singh, A. K., (2014), pentahexoctite: A new two-dimensional allotrope of carbon, Scientific reports, 4(1), 7164.

[22] Shegehalli, V. S. and Kanabur, R., (2015), Arithmetic-geometric indices of path graph, J. Math. Comput. Sci-JM, 16, pp. 19-24.

[23] Some, B. and pal, A., (2025), Sombor index of fuzzy graph, TWMS J. App. and Eng. Math., 15(6), pp. 1325-1346.

[24] Sun, H., Peng, J., Zhao, K., Usman, R., Khan, A. and Wang, M., (2017), Efficient luminescent microtubes of charge-transfer organic cocrystals involving 1, 2, 4, 5-tetracyanobenzene, carbazole derivatives, and pyrene derivatives, Crystal Growth & Design, 17(12), pp. 6684-6691.

[25] Vukivevic, D. and Furtula, B., (2009), Topological index based on the ratios of geometrical and arithmetical means of end-vertex degrees of edges, J. Math. Chem., 46, pp. 1369-1376.
[26] Wang, Z., (2018), Large n-heteroacene derivaties: synthesis, characterization and application as n-type and ambipolar semiconductos (Doctoral dissertation).
[27] Ye, A., Javed, A., Jamil, M. K., Abdul Sattar, K., Aslam, A., Iqbal, Z. and Fahad, A., (2020), On computation of face index of certain nanotubes, Discret. Dyn. Nat. Soc., 2020(1), 3468426.
[28] Yogalakshmi, K. and Easwaramoorthy, D., (2024), A New Approach for Generalized Fractal Dimensions Based on Topological Indices for Pyracyclene and Pentahexoctite Networks, IEEE, 12, pp. 166176-166187.
[29] Zong, L., (2012), The harmonic index for graphs, Appl. Math. Lett., 25(3), pp. 561–566.

H. T. Sharathkumar is a research scholar in the Department of Studies and Research in Mathematics, Tumkur University, Jnanasiri Campus, Tumakuru, Karnataka, India. He completed his Masters in Mathematics at the same department in Tumkur University. His research interest includes graph theory and chemical graph theory, with a key focus on structural graph invariants and their theoretical implications in chemical informatics and network analysis.

Pooja Narasimha is a faculty member in the Department of Mathematics, University College of Science, Tumkur University, Tumakuru. She completed her Masters in Mathematics at Department of Studies and Research in Mathematics, Tumkur University, Tumkur, Karnataka. Her areas of interest in research are Graph coloring particularly Magic sigma coloring and Chemical graph theory.

Narahari Narasimha Swamy is an active researcher working in the domain of graph theory and chemical graph theory. He has a teaching and research experience of over 20 years. He is presently working as the Head of the Department of Mathematics, University College of Science, Tumkur University, Tumakuru, Karnataka, India.

H. M. Nagesh is an active researcher working in the domain of graph theory and chemical graph theory. He has a teaching and research experience of over 20 years. He is presently working as the Associate Professor of Mathematics, PES University, Bangalore, Karnataka, India.